Progress in Engineering Application and Technology Vol. 2 No. 2 (2021) 983–1000

PEAT

Homepage: http://penerbit.uthm.edu.my/periodicals/index.php/peat
e-ISSN : 2773-5303

Effect of Air and Steam on The Performance of Syngas Yield Using Downdraft Gasification Method

Siti Syafrina Nurhidayah Shamsuddin[1], Nor Afzanizam Samiran[1]*

[1]Department of Mechanical Engineering Technology, Faculty of Engineering Technology,
Universiti Tun Hussein Onn Malaysia, Pagoh Johor, 84600 MALAYSIA

DOI: https://doi.org/10.30880/peat.2021.02.02.089
Received 13 January 2021; Accepted 01 March 2021; Available online 02 December 2021

Abstract: Considering shifts in the global climate, there is an opportunity to diversify from fossil fuels as part of measures to minimize greenhouse gas emissions. As an energy source, biomass has the potential to generate sustainable energy and fuels and to contribute to a cleaner future. Utilizing biomass as a carbon dioxide neutral organic source in an integrated system effectively produces useful goods and reduces waste and non-renewable resource usage. Gasification, the preferred method for biomass conversion into fuel gas, offers greater electrical efficiencies than combustion, making it possible to use the syngas produced by the gasification process to generate clean energy. In addition, syngas can also be used for ammonia and methanol production, thus reducing their respective natural gas dependencies. This study will detail the biomass gasification process considering the type of gasifier and various gasifying agents. To achieve this aim, an ANSYS Fluent simulation model is developed to analyze the effect of various gasification agents on the performance of syngas yield and temperature distribution. The comparative analysis between the single-stage and two-stage downdraft reactor is performed to study the influence of air as gasifying inlet corresponding in comparison with steam and air for primary and secondary ports of gasifying inlet. Based on the results and discussion, the two-stage downdraft reactor utilizes the maximum production rate of syngas yield composition with temperature distribution in the range of 350-2000K along the gasifier. This shows the increase in temperature has a positive impact on the quality of syngas produced and the performance of the gasification process.

Keywords: Biomass Gasification, Gasification Agents, Computational Fluid Dynamic (CFD)

1. Introduction

Throughout the past years, worldwide demand for energy has grown tremendously. The current annual level of global energy consumption is 533 EJ and is anticipated to expand by 41.00 % in 2035. This rapid growth means extreme variations in the cost of fossil energy, and drastic change in the

*Corresponding author: afzanizam@uthm.edu.my

scenario of renewables (Martínez et al., 2020). Biomass is identified as the major energy source and the biggest possible alternative of replacing fossil fuels that could satisfy fuel supply in the future sustainability. As such, biomass is even classed as 4th rank largest energy source after coal, oil, and natural gas, and holds 14.00 % of the world 's final energy consumption in 2014 (Situmorang et al., 2020). Challenged on the need for waste disposal and the rising energy demand, biomass gasification is a promising technological choice that has attracted attention from the scientific community because of its benefits in terms of easy handling, raw material, high performance, and synthesis gas production with an adequate standard for thermal or power generation applications. During gasification, biomass is transformed into syngas, which is mainly comprised of carbon monoxide (CO), hydrogen (H_2), carbon dioxide (CO_2), methane (CH_4), nitrogen (N_2), water (H_2O), as well as some proportions of hydrocarbons such as ethylene (C_2H_4) and ethane (C_2H_6). Synthesis gas or syngas can then be used to generate thermal or electrical energy in devices such as internal combustion engines (ICEs), fuel cells, or gas turbines, after a conditioning process (Martínez et al., 2020).

The type of biomass waste, gasifier, and gasifying agent influences the composition of biomass-derived syngas. Various gasification agents such as steam, oxygen, air, and oxygen-enriched air can be used for the gasification process resulting in a distinct syngas composition (AlNouss et al., 2020). Although different kinds of gasifiers such as moving bed, entrained flow, and fluidized beds have been broadly used in industry and studied throughout scientific literature, extensive research activities are continuing for technology development and enhancement (de Sales et al., 2017). Because of its higher efficiency compared to other thermochemical processes such as pyrolysis, direct combustion, and liquefaction, downdraft gasification has been proven to be the best option for small to medium-sized throughputs (Yao et al., 2018).

While biomass-based power and hydrogen production plants have become widely known in previous years and a lot of studies have been dedicated to this research area, there is limited study focusing on using different gasification agents and contrasting their significant effect on the producer gas and the gasification process. The present paper aims to study and compare the performance of the gasification process employing various gasification agents in a single-stage and two-stage downdraft reactor. Although there are numerous works on biomass gasification on recent literature studies, no many works are found using the two-stage downdraft reactor. Both of the reactors are designed for simulation of the gasifier and the effects of different types of gasifying agents are being evaluated.

2. Methodology

2.1 Reactor Design

In this research, single-stage and two-stage downdraft gasifiers were performed to determine the effects of producer gas due to steam and air as their gasification agents (Figure 1 and Figure 2). Input delivery of the gasifying agent was performed through four injection nozzles, arranged in a radial 90 º pattern. Both of the reactors have an injection nozzle internal diameter of 0.07 m and an elevation of 1.75 m (from the top of the reactor to the ashtray). These gasifier models are designed by using Solidworks and the details of these gasifiers can be discovered in Table 1.

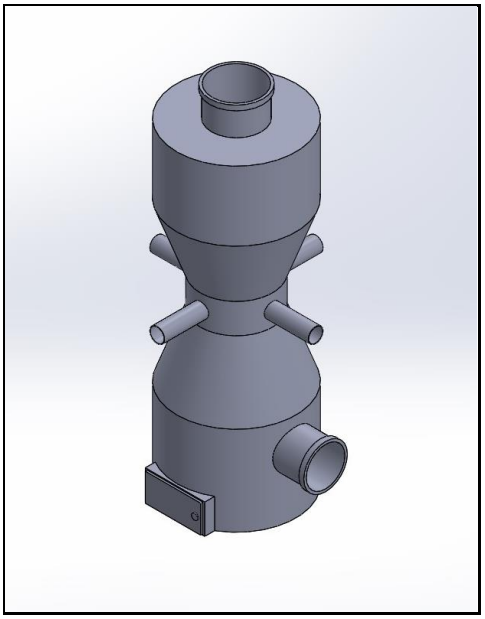

Figure 1: Single-stage downdraft gasifier (Model 1)

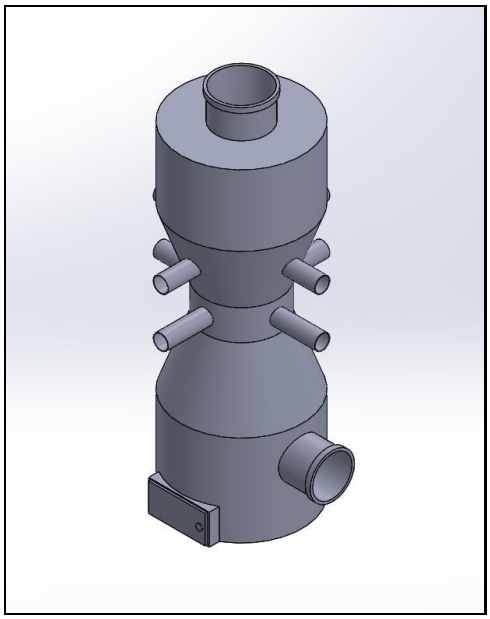

Figure 2: Two-stage downdraft gasifier (Model 2)

Table 1: Dimension of gasifier

Part of Gasifier	Dimension (m)
Height of gasifier	1.750
Throat diameter	0.333
Thickness of shell	0.015
Injection nozzle diameter	0.070
Feedstock inlet diameter	0.245
Syngas outlet diameter	0.195

Only for the two-stage downdraft gasifier, the first stage is 0.945 m above the grate whereas the second stage is 0.245 below the first inlet. The basic concept of making two different points for feeding the gasifying agent is to isolate the pyrolysis zone from the reduction zone to achieve substantial reductions of the tar concentration. Thus, the primary port of the gasifying agent is located near the top of the reactor (just in the drying and pyrolysis zones) to increase the temperature in those regions when supplying steam. The second port is in the centre of the reactor, specifically in the oxidation region, where temperature rises due to the complete oxidation of these volatiles and their transformation into CO_2 and H_2O and lighter compounds as a result. Finally, this gas stream (syngas) flows through the bottom of the reactor where the mixture of unconverted carbon and ash, promotes its cleaning (de Sales et al., 2017).

2.2 Computational Simulation

The use of computational methods to simulate real problems is of great benefit today due to the reduction of construction costs, providing the possibility to test various geometries and fuels in the case of gasifiers without actually constructing a reactor and possessing the fuels. But computational model has to be accurate for that, so it has to be compared with actual experimental results, and if it gives PCI's final values very similar when comparing, it can be assumed that the mathematical model employed can be used to promote and speed up future projects. Hence, ANSYS Fluent was used for this analysis with the boundary conditions and simulation strategy (Frigo et al., 2019).

2.3 Governing Equations

There are currently primarily two types of methods used for CFD simulations of biomass gasification, the Eulerian-Lagrangian approach and the Eulerian-Eulerian approach. The Navier-Stokes equations describe the gas phase, in the Eulerian-Lagrangian method, while the solid phase is handled as a discrete phase. Meanwhile, the Eulerian-Eulerian solution needs less computation, since it views the solid process as a continuum. Newton's Laws of Motion determines the trajectory of each particle and the particle collisions are represented by the soft-sphere or hard-sphere model. Other variables such as temperature and gas concentration are determined for each particle by the energy equations and mass transfer. Because each particle in the system is monitored, the precision of the simulation outcome can be increased, but this method inevitably often requires a large amount of computational resources (Frigo et al., 2019). As for this simulation study, the equations governing the system are mass conservation, moment conservation, energy equation, transport equation and species transport model shown in Eq. 1, Eq. 2, Eq. 3, Eq. 4, and Eq. 5.

2.3.1 Mass Conservation Equation

The general form of the mass conservation equation, known as the continuity equation, is as follows:

$$\frac{\partial \rho}{\partial t} + \nabla \cdot (\rho \vec{v}) = S_m \qquad Eq.\,1$$

where S_m is the mass added to the continuous phase from the dispersed second phase (Prasertcharoensuk et al., 2018).

2.3.2 Momentum Conservation Equation

The momentum equation, premised on Newton's laws of motion, refers the total amount of the forces acting on the fluid element to its acceleration, which is the rate of the change of momentum in the direction of the resulting force. The following term can be used to write the momentum conservation equation:

$$\frac{\partial(\rho\vec{v})}{\partial t} + \nabla \cdot (\rho\vec{v}\vec{v}) = -\nabla \cdot p + \nabla \cdot (\vec{\tau}) + \rho\vec{g} + \vec{F} \qquad Eq.2$$

where ρ is the static pressure, $\rho\vec{g}$ and $\vec{F}$ are the gravitational body force and external body force respectively (Prasertcharoensuk et al., 2018). Also, $\vec{\tau}$ refers to stress tensor.

2.3.3. Energy Conservation Equation

Energy conservation is derived on the first law of thermodynamics, the internal energy generated by the system must be equal to the heat absorbed by the system minus the work performed by the system. It can be described as follows in the general form:

$$\frac{\partial}{\partial t}(\rho E) + \nabla \cdot \left(\vec{v}(\rho E + \rho)\right) = \nabla \cdot \left(k_{eff}\nabla T - \sum_{j=1}^{N} h_j \vec{J}_j + (\tau \cdot \vec{v}) \right) + S_h \qquad Eq.3$$

where k_{eff} is the effective thermal conductivity (k + k_t, where k_t is the turbulent thermal conductivity) (Prasertcharoensuk et al., 2018). The first three terms of the right-hand side of the Eq. 3 represent heat flux due to the conduction according to Fourier's law of conduction, species diffusion and viscous dissipation due to normal shear stresses respectively.

2.3.4 Transport Equation for Standard k-Epsilon

The standard k-ε model is among the most used turbulence models in Computational Fluid Dynamics due to its robustness and acceptable accuracy for a wide range of flows. The k- ε model is a semi-empirical model based on the turbulent kinetic energy k and its dissipation rate ε transport equations. It is presumed that the flow is completely turbulent in the derivation of the model, and the effects of molecular viscosity are negligible. The kinetic energy transport equations and their rate of dissipation are defined as follows:

$$\frac{\partial}{\partial t}(\rho k) + \frac{\partial}{\partial x_i}(\rho k u_i) = \frac{\partial}{\partial x_j}\left[\left(\mu + \frac{\mu_t}{\sigma_k}\right)\frac{\partial k}{\partial x_j}\right] + G_k + G_b - \rho\varepsilon - Y_m + S_k \qquad Eq.4$$

where S_k is the source terms for k and ε, and G_k is the term for the production of turbulent kinetic energy due to the mean velocity gradient (Prasertcharoensuk et al., 2018).

2.3.5 Species Transport Model

The species model is a great way for biomass gasification modelling. The transport model for the species was chosen to model the chemical reactions within the gasifier and to determine the composition of different species, such as CO, CO_2, H_2, N_2, and CH_4. For each species, the common form of the transport equation is known as

$$\frac{\partial}{\partial t}(\rho Y_i) + \nabla(\rho\vec{v}Y_i) = \nabla\vec{J}_i + R_i \qquad Eq.5$$

where R_i is the net rate of production of species *i* by chemical reaction (Gupta et al., 2017).

2.4 Reactions Model

Four different processes take place in gasification. First, the feedstock is dried, a phase in which the moisture content of the feedstock is evaporated. Next, the feedstock reaches the stage of pyrolysis. Oxygen is choked during pyrolysis to avoid combustion, and high temperatures encourage biomass to decompose into useful chemicals. In order to supply heat to the gasification, drying and pyrolysis zone, the feedstock then enters the combustion zone where the feedstock is partially combusted. Last, the feedstock reaches the reduction zone in which hydrocarbon gases, oils, and charcoal are converted into

raw materials (Enget & Jaojaruek, 2020). Figure 3 illustrates these processes and their positions in the downdraft gasifier.

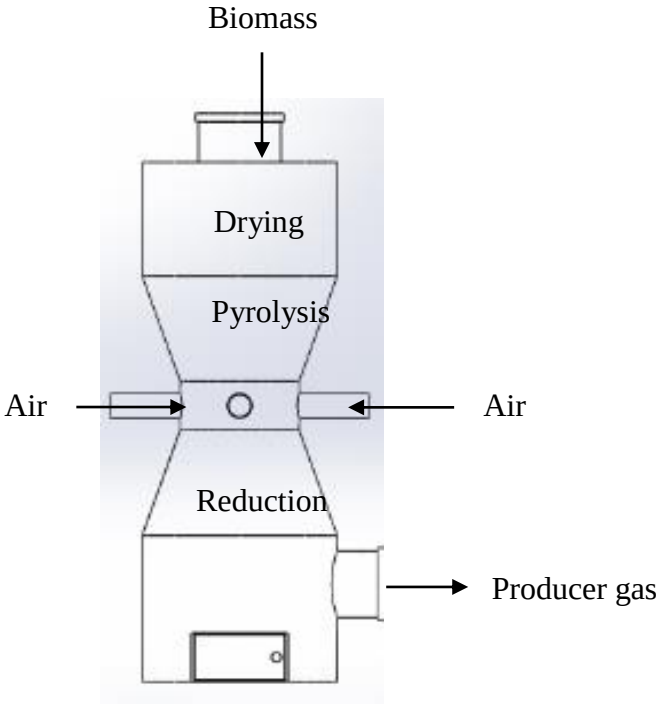

Figure 3: Throated downdraft gasifier diagram

2.4.1 Pyrolysis Zone

Pyrolysis, in the absence of oxygen/air at a temperature range of 473-773 K, is the thermochemical decomposition of feedstock into condensable and non-condensable gases and carbon. The total pyrolysis decomposition can be represented in Figure 4.

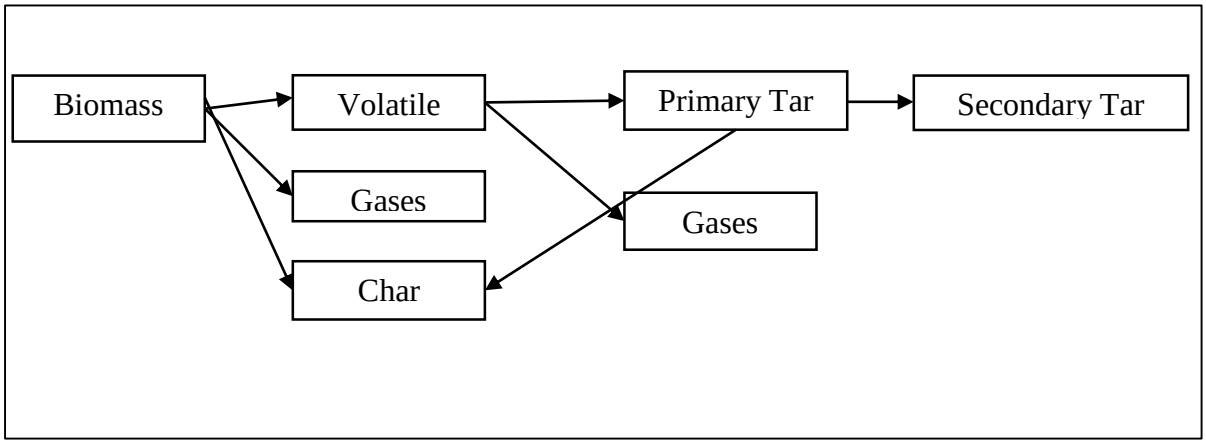

Figure 4: Pathways of reaction in the pyrolysis process

To represent the exact mechanism of the pyrolysis process, there is restricted kinetic reaction data found in the literature. This is probably due to the greater number of potential reactions in the pyrolysis zone from which tars can be formed. Tars are a diverse mixture of condensable hydrocarbons comprising several single aromatic ring compounds with and without complex aromatic polyclinic hydrocarbons (PAHs). To model the reactions of the pyrolysis processes proposed by previous researchers, a simplified one-step global reaction model has been widely adopted. To simplify the model, this model predicts that all volatile and tar compounds at the pyrolysis phase are instantaneously

further decomposed into CO, CO_2, CH_4, H_2, and H_2O compounds. Kinetic parameters for pyrolysis, e.g., 1.00×10^8 s^{-1} and 140 $kJmol^{-1}$ were for pre-exponential and activation energy (Prasertcharoensuk et al., 2018).

2.4.2 Oxidation Zone

The oxidation zone is where, at temperatures between 1373 and 1773 K, reactions between the char from the pyrolysis stage and the gasifying agent (O_2, CO_2, air or steam) occur to produce most of the CO, H_2O and CO_2. With their kinetic reaction rate parameters used in the model, three major reactions in the oxidation zone are considered (Prasertcharoensuk et al., 2018).

$$C + O_2 \rightarrow CO_2 \qquad (\Delta H^o = -394\ kJmol^{-1})$$

$$C + \tfrac{1}{2}O_2 \rightarrow CO \qquad (\Delta H^o = -111\ kJmol^{-1})$$

$$H_2 + \tfrac{1}{2}O_2 \rightarrow H_2O \qquad (\Delta H^o = -242\ kJmol^{-1})$$

2.4.3 Reduction Zone

In this region, in the temperature range of 973-1273 K, the remaining residues and gaseous products from the pyrolysis and oxidation zones are converted into non-condensable gases (CO, CO_2, CH_4, H_2,), including heterogeneous and homogeneous reactions. In the reduction zone, five reactions are considered as follows, as well as the kinetic reaction rate parameters used in the model (Prasertcharoensuk et al., 2018).

$$C + CO_2 \rightleftharpoons 2CO \qquad (\Delta H^o = +172\ kJmol^{-1}) \qquad \text{(Boudouard reaction)}$$

$$C + H_2O \rightarrow CO + H_2 \qquad (\Delta H^o = +131\ kJmol^{-1}) \qquad \text{(Steam reforming reaction)}$$

$$C + 2H_2 \rightleftharpoons CH_4 \qquad (\Delta H^o = -74.8\ kJmol^{-1}) \qquad \text{(Hydrogenation reaction)}$$

$$CH_4 + H_2O \rightarrow CO + 3H_2 \qquad (\Delta H^o = +206\ kJmol^{-1}) \qquad \text{(Steam reforming reaction)}$$

$$CO + H_2O \rightleftharpoons CO_2 + H_2 \qquad (\Delta H^o = -41.2\ kJmol^{-1}) \qquad \text{(Water-gas shift reaction)}$$

2.5 Grid Setup

In order to measure structure parameters with greater precision, meshing is a method used to fragment a structure into smaller parts. A finite number of grid points inside the structure called nodes are generated during meshing. For the desired parameters, governing equations are solved numerically at these nodes. Section 2.3 defined the governing equations solved at the nodes in this model. For solving these equations, the finite volume method is used. The greater the meshing density, the greater the problem-solving precision. Higher precision, however, comes at the expense of greater complexity in solving equations. Meshes must therefore be generated in a balance with adequate density to collect the most important data, but with a relatively low density, where the equations can be solved in a timely manner by the software (Enget & Jaojaruek, 2020). In this present study, capture curvature is the size function for the meshing process. Meshing of model is shown in the Figure 5 and Figure 6 with the details in the Table 2.

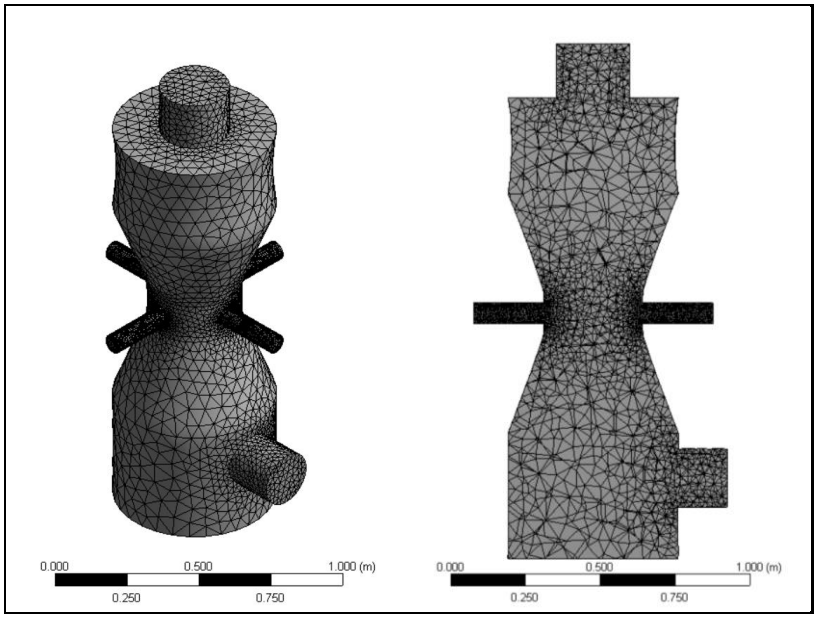

Figure 5: Meshing of Model 1 in predominantly tetrahedron cell

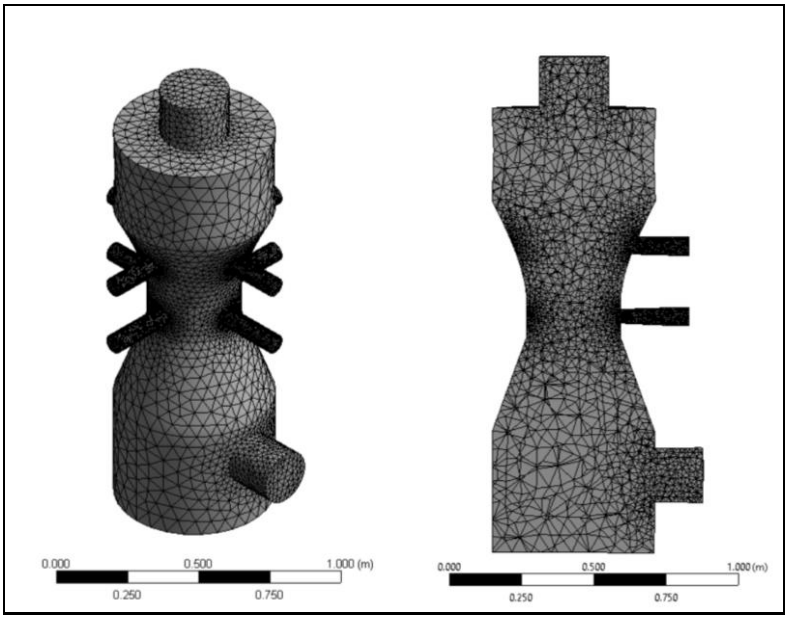

Figure 6: Meshing of Model 2 predominantly tetrahedron cell

Table 2: Meshing details

Description	Model 1	Model 2
Growth Rate	1.2	1.2
Capture Curvature	12.0º	12.0º
Smoothing	High	High
Mesh Metric	Skewness (Max Value: 0.79017)	Skewness (Max Value:0.79906)
Inflation Option	Smooth Transition	Smooth Transition
Transition Ratio	0.272	0.272

Nodes	22807	37965
Elements	113428	190015

2.6 Boundary Conditions

The following assumptions were made to streamline the simulation of a throat downdraft gasifier (Prasertcharoensuk et al., 2018):

i. Atmospheric pressure.
ii. The gasifier was operated under steady state condition.
iii. No heat loss through the vessel wall.
iv. No slip boundary condition at the wall of the gasifier. The wall was assumed to be insulated and the heat flux at the wall was neglected.
v. The wood feed rate was 12 kg/hr at a temperature of 350 K.
vi. The gasification agent (air and steam) was introduced through nozzles at 660 K with a mass flow rate of 20 kg/hr.
vii. The turbulence intensity is set to 5.00 %.

2.7 Simulation Strategy

ANSYS Fluent Computational Fluid Dynamic (CFD) software was used in this analysis for numerical simulation. The simulation setup was conducted in ANSYS Fluent were consists of geometry development, geometry import and meshing, CFD pre-processing, solving CFD simulation, and CFD post-processing. The geometry in ANSYS Workbench was described as a poly solid after it was built in Solidworks. The model was meshed with the forms of tetrahedron cells using ANSYS Mesh, and the setup process started by setting the gravitational force at 9.81 ms^{-2} on the y-axis. The solver preferences were defined at Fluent. With possible near-well treatment, a K-ε turbulence model was developed. Thus, the realizable k-ε model was used in this simulation analysis to capture the turbulence flow of the gas phase within the gasifier with the standard wall function.

The model of species was described for species transport and volumetric reaction was applied. Moreover, the rates of the species were determined using the Eddy-dissipation model. The reaction fuel (waste wood) is described in accordance with the proximate and ultimate analysis. Wood injection utilizes a discrete phase with a uniform type of combusting particles. Then, it defines all the boundary conditions and the set of parameters listed in Table 3. To solve the pressure-velocity coupling, the SIMPLE algorithm scheme was used and the standard scheme was chosen for the pressure discretization. After grid independence studies were completed, the second-order upwind scheme was introduced to obtain precise results for other measured variables. Finally, using standard initialization, the simulation configuration was initialized and the calculation was run with an iteration number of 1000.

Table 3: Parameters used for simulating a gasifier for throat downdraft

Biomass Characterization (de Sales et al., 2017)	
Analysis	Value
Ultimate (wt%) on dry-ash-free(daf) basis	
Carbon	49.0
Nitrogen	0.20
Hydrogen	6.30

Sulfur	0.10
Oxygen	44.40
Proximate (wt%) on dry basis	
Ash	0.79
Volatile matter	72.86
Fixed caron	15.18
Heating value (kJ/kg) on dry basis	
HHV	19744.3
LHV	18389.9

Zone	Boundary Type	Value	Temperature
Feedstock inlet	Mass flow inlet	12 kg/hr	350 K
Air inlet	Mass flow inlet	20 kg/hr	660 K
Steam inlet	Mass flow inlet	20 kg/hr	660 K
Syngas outlet	Outflow	-	-
Gasifier wall	Wall	0 Wm^2	-
Solution Methods			
Pressure-Velocity Coupling	SIMPLE		
Gradient	Least Square Cell Based		
Pressure	Standard		
All other parameters	Second Order Upwind		
Solution Controls			
Direct Specification Method	Normal to Boundary		
Turbulence Specification Method	Intensity and Hydraulic Diameter		
Turbulent Intensity	5%		
Solution Initialization			
Initialization Method	Standard Initialization		
Run Calculation			
Number of Iterations	1000		

3. Results and Discussion

3.1 Temperature Distribution in Gasifier

Temperature distribution along the gasifier centreline is shown in Figure 7, where the temperature in the gasifier increases along the height from the top. The drying zone is positioned at the top followed by phases of pyrolysis and oxidation and a change in temperature is observed down the gasifier. The temperature contour in Table 4.1 indicates the locations denoted in the graph according to the colour of the legend view. Corresponding to the temperature graph of Model 1, it goes slightly increases from the drying zone to the reduction zone and reaches the highest point at the oxidation zone (660 K) where the combustion of char from the pyrolysis stage and the gasifying agent (air) occurs to produce most of the CO, H_2O and CO_2. Based on this study, it is found that the temperature range for the single-stage reactor is 350-660 K. However, in the temperature curve of Model 2, the reaction is gradually spiking and relatively fluctuates during the pyrolysis and oxidation zones since air and steam as the gasifying agents are supplied. For the two-stage downdraft gasifier, steam is fed at the pyrolysis stage whereas air is fed during the oxidation stage. The temperature of both pyrolysis and oxidation zone are dropping by at least 100 K and maximum drop in temperature is observed of 700 K. The fluctuation appearances indicate that the effects of the oxidation zone temperature are instantly detected, although steam is introduced in the pyrolysis zone. It is apparently due to the accumulation of steam supply and the temperature of the drying zone is considerably higher than the temperature of the supplied steam (Sharma & Sheth, 2016).

Table 4: Temperature contour of gasifier

	Model 1	Model 2
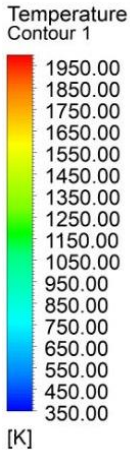		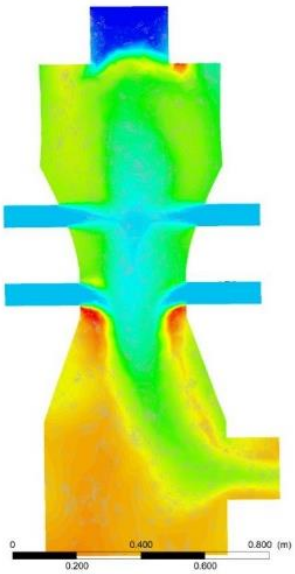

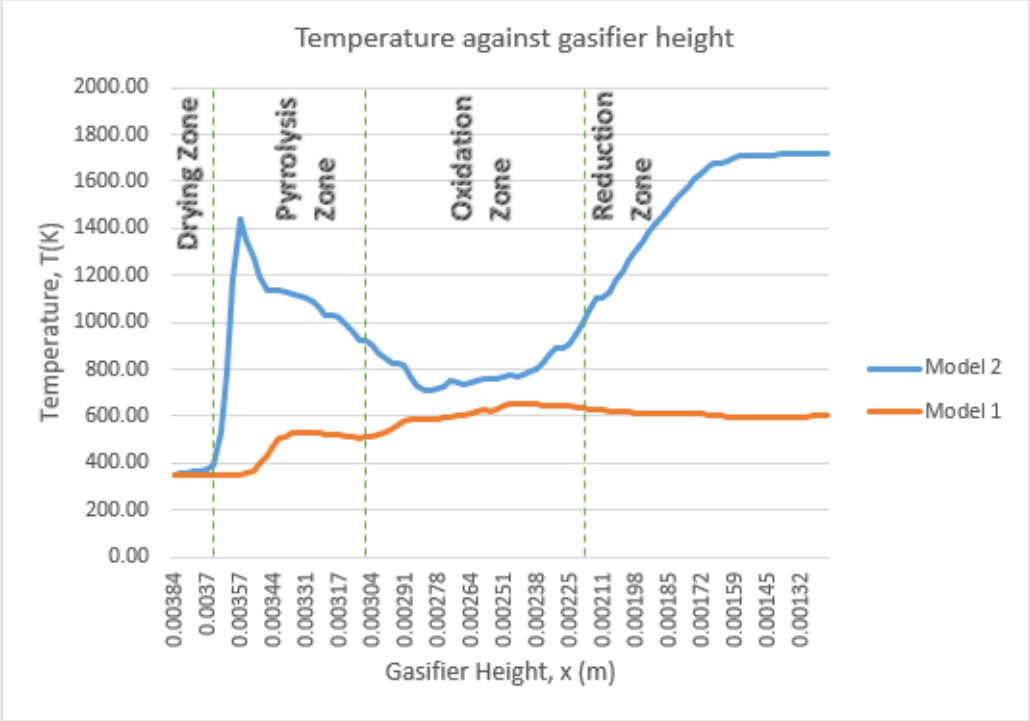

Figure 7: Temperature distribution along the gasifier centreline in both single-stage and two-stage downdraft reactor

The temperatures of the pyrolysis and oxidation zone depends on heat emitted from the oxidation zone when the gasifier is worked on the only one-stage gasifying agent supplied, wherein this case, the one-stage employing air as its gasifying medium. By installing a second stage gasification inlet just above the normal point, the temperature in the drying and reduction areas can increase and not only be benefitted by the combustion heat produced in the region of oxidation (Lisbeth et al., 2014). (Kalinci et al., 2009) reported that the temperature of gasification not only influences the output of the product but also controls the energy input process. A gas mixture of H_2 and CO with small volumes of CH_4 and higher hydrocarbons is generated at a high gasification temperature, especially between 800 and 850 °C. Strong carbon (C(s)) and CH4 in the product gas are present at low temperatures. In actual gasifiers, solid carbon is transported to the catalytic bed and thus deactivated at active catalyst sites. The product gas needs to be made free of solid carbon.

3.4 Syngas Yield Composition

Various gasifying media could be used to gasify biomass, the choice of which depends on the composition of the product gas and energy considerations. H_2 and CO are the two most significant gas species in gaseous products for biomass air gasification and steam gasification, the content and ratio of which are two benchmarks for evaluating gas efficiency (Lv et al., 2007). Nevertheless, due to obstacles during the simulation work to produce the composition of H_2 in producer gas, this analysis consists of CO composition only. Table 5 demonstrates the gas formation between biomass air gasification (Model 1) and biomass steam and air gasification (Model 2) in the downdraft reactor.

Table 5: Contour of syngas composition

	Model 1	Model 2
CO	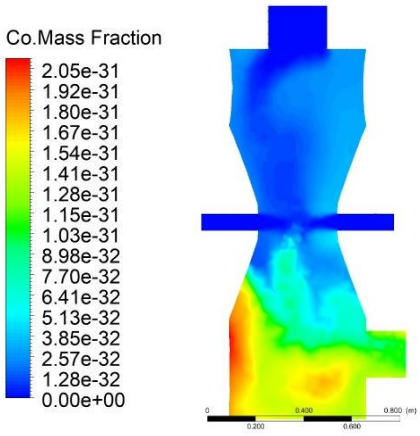	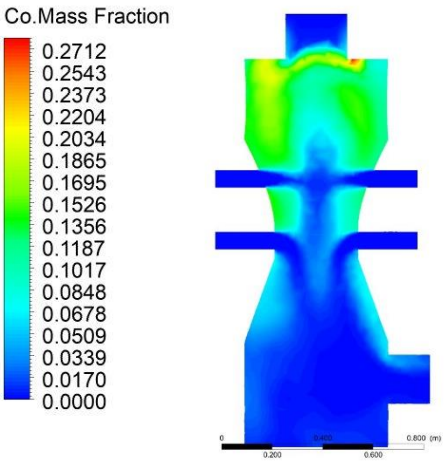
CO_2	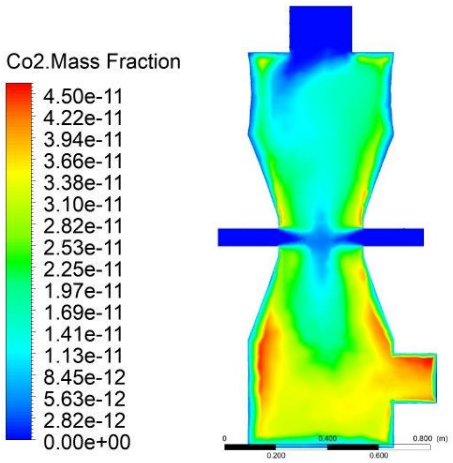	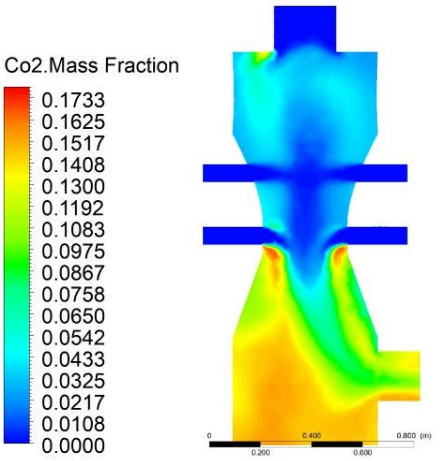
H_2O	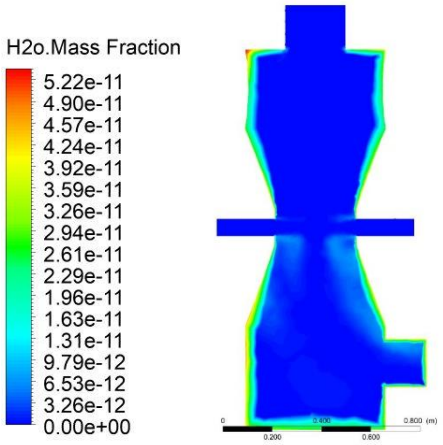	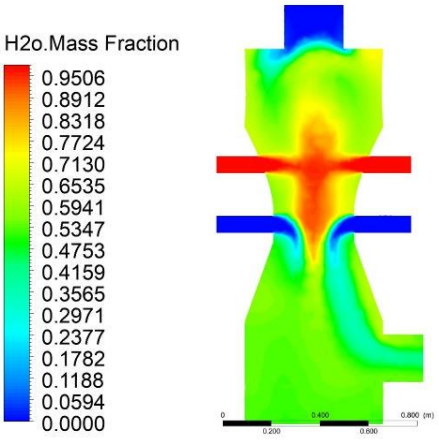

N_2	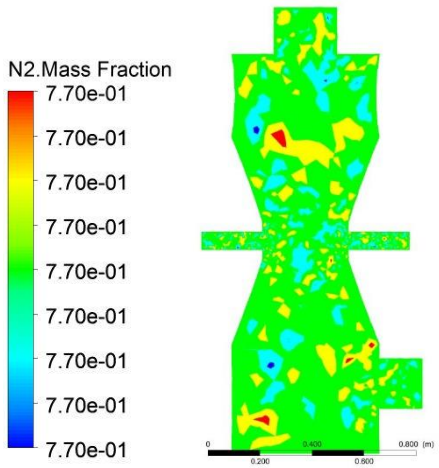	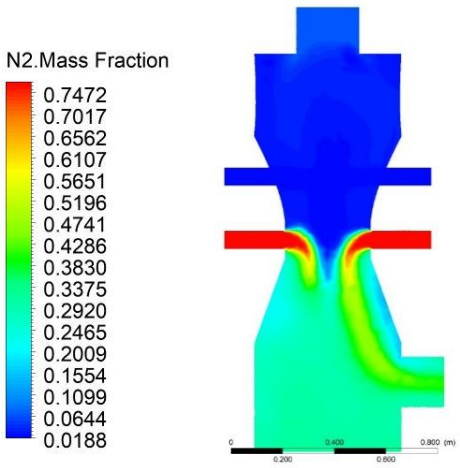
O_2	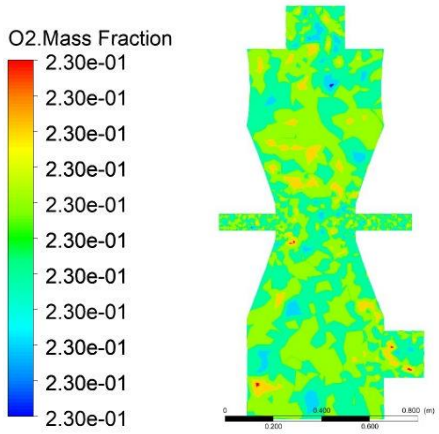	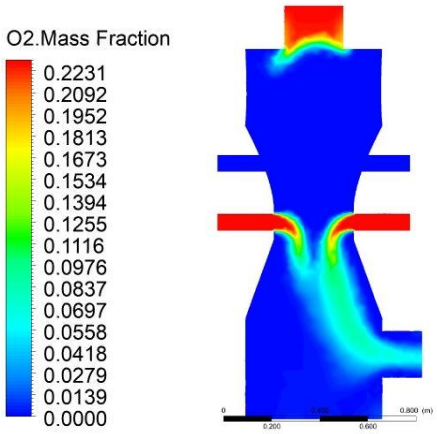

Based on the contour of syngas composition, the contour of the two-stage downdraft reactor is well-presented compared to the contour of the single-stage downdraft gasifier. This can be proven with the vector of velocity for both gasifiers in Table 6. In the pyrolysis and drying zone, the vector of velocity demonstrates the pyrolyzed gas and moisture produced downwards. In the zone where gasification media are supplied from the injection nozzles, biomass is being fed to the gasifier and oxidized. The pyrolyzed gases pass into a combustion zone and heat is transferred into the pyrolysis and drying zone through the combustion area. The temperature of the biomass particles that rest above the oxidation zone is increased by the released thermal energy from the biomass combustion (Sheth & Babu, 2009).

Table 6: Vector velocity

Model 1	Model 2
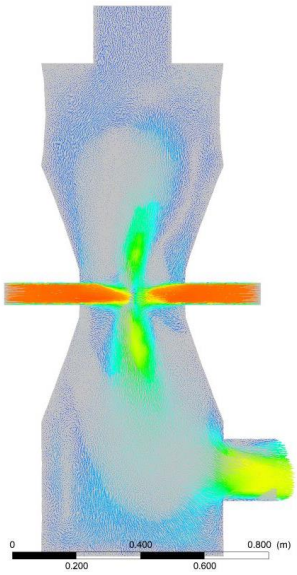	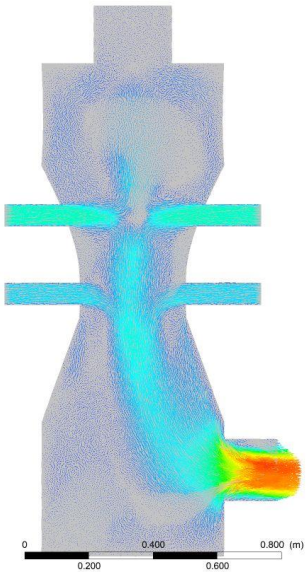

Tar is undeniably the biggest technical barrier, considering its high viscosity and molecular weight physical and chemical characteristics which make it almost impossible for direct use of gases in thermal engines. Thus, the removal of tar is a crucial technical task; the removal of tar can be divided into two groups: primary processes for cleaning using the gasifier, and secondary processes for gas cleaning using a secondary procedure after the gasification phase. In the perspective of the primary method of removal of the tar in conjunction with a thermal cracking (a process of high temperatures in the breakdown of tar compounds), a two-stage gasification system was established based on the injection into a combustion zone and at a different location, that is, in the pyrolysis zone which led in that region to the partial oxidation of the biomass (Lisbeth et al., 2014).

It is simple and easy to understand the difference between air gasification and steam-air gasification in Figure 8. Each mass species is defined by the function calculator in the ANSYS Fluent to extract the maximum value of species at the syngas outlet. In the contrast between one-stage and two-stage gasifier, there is a growing trend in the fraction CO and H_2O just opposite nitrogen, where the single-stage reactor produces more nitrogen than the double-stage reactor (Sharma & Sheth, 2016). Since the amount of CO_2 production in the combustion zone is also greater, biomass air gasification offers a higher quantity of N_2. The conversion of CO_2 into CO, meanwhile, depends on the rate of reactions in the reduction zone and the length of the reduction zone. For biomass steam and air gasification, the gasifying agent inlet was divided into primary and secondary ports for the simulation work. The relation between primary and secondary inlet is to find the influence of steam and air on the gasification process. The result is supported by these findings as the presence of steam lowers the gas flow, resulting in a deeper reforming reaction of biomass gasification gases, thereby producing more CO (Lv et al., 2007).

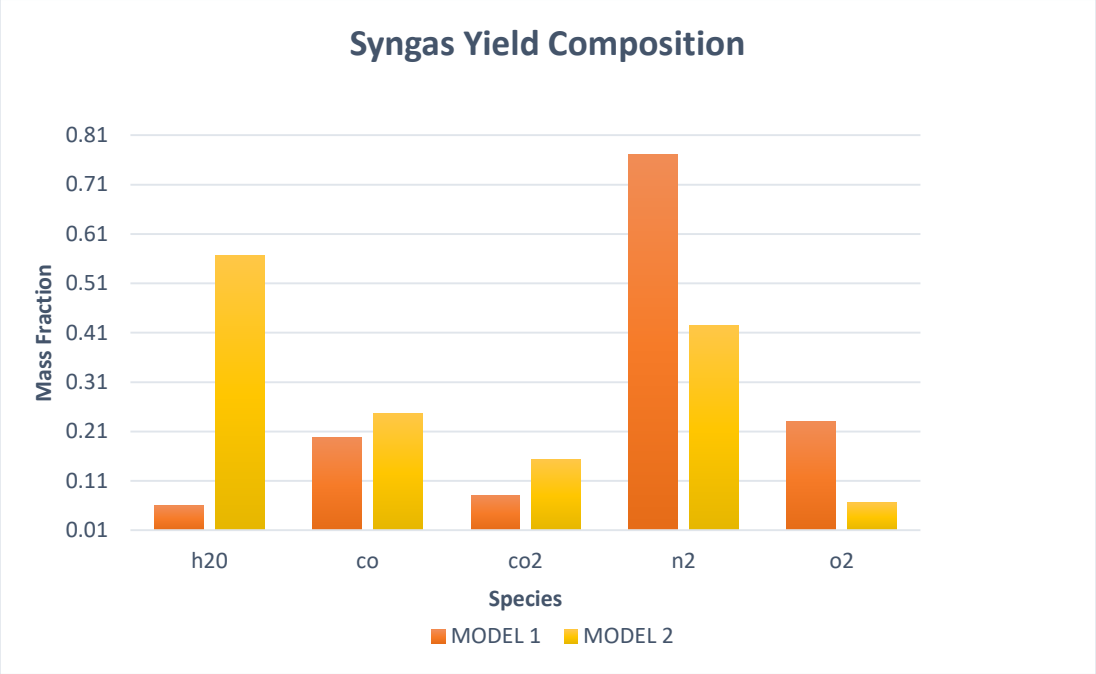

Figure 8: Comparison of the composition of syngas yield between single and two-stage reactor downdraft reactors

From this simulation study, the two-stage downdraft reactor shows a higher production rate of water vapor (H_2O) and carbon monoxide (CO) compared to the single-stage that only gives a high value of rate for nitrogen (N_2) production. This justified why commercial and research gasifiers generally use steam and air as the gasifying media. The exothermic method of air gasification is low heating gas rich in CO with small quantities of H_2 and higher hydrocarbons. Steam gasification is an endothermic operation, on the other hand, which generates a medium heating value of gas (Kalinci et al., 2009). The highest amount of hydrogen, which is substantially greater than the value for air in a case when steam is used as a gasification agent, is produced. This is because the nitrogen fraction is zero during steam gasification, which results in a change in the chemical balance of the gasification reaction and an increase in the hydrogen content.

Also, the development of the primary and secondary gasifying inlet promotes maximum value of gas yield at the end product. (Nakyai et al., 2017) examined through an exergoeconomic analysis to analyze the effects of the air mixture and air-steam mixture for biomass gasification with/without methane feeding rate. The results showed that the use of air-steam biomass as the co-feeding agent provides the lowest unit hydrogen cost of $2.69 per kilogram. (Jaojaruek et al., 2011) also investigated the use of eucalyptus biomass as fuel in a downdraft gasification with two-stage air supplies, which led to an increase in CO concentration and decreases in CH_4 concentration compared to the downdraft gasifier with a single-stage air supply. For that reason, it was determined with the double-stage of gasifying inlet achieve maximum production rate of syngas yield.

4. Conclusion

In order to limit emissions of GHGs and minimize dependency on fossil fuels, a global emphasis has been put on further incorporation of renewable energy within the global energy mix. Biomass, a CO_2 neutral fuel, as a possible source of energy for valuable chemical and renewable power production. Gasification is also a leading process for creating clean and less polluting intermediate gas for high-efficiency generation, among other methods of thermochemical conversion. However, the gasification process can be carried out with several gasification agents including steam, oxygen, air, and oxygen-enriched air, resulting in a different composition of the produced syngas (AlNouss et al., 2020).

The present study proposed a gasification simulation for the single-stage and two-stage downdraft reactor to study the influence of employing air as the gasification agent for the single-stage gasifier whereas steam and air as the gasification agent for the two-stage reactor. The simulation model was validated by comparing the syngas composition of gasification simulation by using the same parameters and gasification fuel. An overview of gasifier functioning is provided by the simulation study related to temperature changes and the composition of syngas. The simulation study has shown that air gasification yields a higher amount of N_2 since the CO_2 production in the combustion zone is greater. Meanwhile, this study highlighted that steam and air gasification by using the two-stage downdraft reactor produce a maximum production rate of water vapor (H_2O) and carbon monoxide (CO). The findings of the comparison between the studies show that biomass air-steam gasification has an advantage in reducing the efficiency of syngas. The question seems to be that the hydrogen and carbon monoxide contents of gaseous materials tend to be low for this technical method. This problem can be solved by additional CO-shift reactions in a downstream reactor that can be used to maintain the temperature of the necessary reactions at the very high level of the gas at the exit of the downstream gasifier (Lv et al., 2007).

Acknowledgement

The authors would like to thank the Faculty of Engineering Technology, Universiti Tun Hussein Onn Malaysia for its support and providing necessary research facilities for this study.

References

[1] AlNouss, A., McKay, G., & Al-Ansari, T. (2020). A comparison of steam and oxygen fed biomass gasification through a techno-economic-environmental study. *Energy Conversion and Management*, *208*, 112612. https://doi.org/10.1016/j.enconman.2020.112612

[2] de Sales, C. A. V. B., Maya, D. M. Y., Lora, E. E. S., Jaén, R. L., Reyes, A. M. M., González, A. M., Andrade, R. V., & Martínez, J. D. (2017). Experimental study on biomass (eucalyptus spp.) gasification in a two-stage downdraft reactor by using mixtures of air, saturated steam and oxygen as gasifying agents. *Energy Conversion and Management*, *145*, 314–323. https://doi.org/10.1016/j.enconman.2017.04.101

[3] Enget, C., & Jaojaruek, K. (2020). CFD modeling of a downdraft gasifier with woodchips used as feedstock. *International Energy Journal*, *20*(1), 39–56.

[4] Frigo, L., Santos, D. J., Salgado, M., & Yepes Maya, D. M. (2019). *Gasification of Alternative Biomass To Generate Power With Support of Cfd and Cad. January*. https://doi.org/10.26678/abcm.cobem2019.cob2019-1557

[5] Gupta, R., Jain, P., & Vyas, S. (2017). CFD Modeling and Simulation of 10KWE Biomass Downdraft Gasifier. *International Journal of Current Engineering and Technology*, *7*(4), 1446–1452.

[6] Jaojaruek, K., Jarungthammachote, S., Gratuito, M. K. B., Wongsuwan, H., & Homhual, S. (2011). Experimental study of wood downdraft gasification for an improved producer gas quality through an innovative two-stage air and premixed air/gas supply approach. *Bioresource Technology*, *102*(7), 4834–4840. https://doi.org/10.1016/j.biortech.2010.12.024

[7] Kalinci, Y., Hepbasli, A., & Dincer, I. (2009). Biomass-based hydrogen production: A review and analysis. In *International Journal of Hydrogen Energy* (Vol. 34, Issue 21, pp. 8799–8817). Pergamon. https://doi.org/10.1016/j.ijhydene.2009.08.078

[8] Lisbeth, A., Silva, E., Viera, R., Melian, V., Yamile, S., & Jae, R. L. (2014). *ScienceDirect Biomass gasification in a downdraft gasifier with a two-stage air supply : Effect of operating conditions on gas quality*. *1*. https://doi.org/10.1016/j.biombioe.2013.12.017

[9] Lv, P., Yuan, Z., Ma, L., Wu, C., Chen, Y., & Zhu, J. (2007). Hydrogen-rich gas production from biomass air and oxygen/steam gasification in a downdraft gasifier. *Renewable Energy*, *32*(13), 2173–2185. https://doi.org/10.1016/j.renene.2006.11.010

[10] Martínez, L. V., Rubiano, J. E., Figueredo, M., & Gómez, M. F. (2020). Experimental study on the performance of gasification of corncobs in a downdraft fixed bed gasifier at various conditions. *Renewable Energy*, *148*, 1216–1226. https://doi.org/10.1016/j.renene.2019.10.034

[11] Nakyai, T., Authayanun, S., Patcharavorachot, Y., Arpornwichanop, A., Assabumrungrat, S., & Saebea, D. (2017). Exergoeconomics of hydrogen production from biomass air-steam gasification with methane co-feeding. *Energy Conversion and Management*, *140*, 228–239. https://doi.org/10.1016/j.enconman.2017.03.002

[12] Prasertcharoensuk, P., Hernandez, D. A., Bull, S. J., & Phan, A. N. (2018). Optimisation of a throat downdraft gasifier for hydrogen production. *Biomass and Bioenergy*, *116*, 216–226. https://doi.org/10.1016/j.biombioe.2018.06.019

[13] Sharma, S., & Sheth, P. N. (2016). Air-steam biomass gasification: Experiments, modeling and simulation. *Energy Conversion and Management*, *110*, 307–318. https://doi.org/10.1016/j.enconman.2015.12.030

[14] Sheth, P. N., & Babu, B. V. (2009). Experimental studies on producer gas generation from wood waste in a downdraft biomass gasifier. *Bioresource Technology*, *100*(12), 3127–3133. https://doi.org/10.1016/j.biortech.2009.01.024

[15] Situmorang, Y. A., Zhao, Z., Yoshida, A., Abudula, A., & Guan, G. (2020). Small-scale biomass gasification systems for power generation (<200 kW class): A review. In *Renewable and Sustainable Energy Reviews* (Vol. 117, p. 109486). Elsevier Ltd. https://doi.org/10.1016/j.rser.2019.109486

[16] Yao, Z., You, S., Ge, T., & Wang, C. H. (2018). Biomass gasification for syngas and biochar co-production: Energy application and economic evaluation. *Applied Energy*, *209*, 43–55. https://doi.org/10.1016/j.apenergy.2017.10.077